Variety of [Fe, N, O] Isomers. A Theoretical Study

Andreas Fiedler and Suehiro Iwata*

Institute for Molecular Science, Myodaiji, Okazaki 444-8585, Japan

Received: December 16, 1997; In Final Form: March 11, 1998

Stationary points on the potential energy hypersurfaces of triatomic [Fe, N, O] have been systematically studied using an economic combination of a density functional/Hartree−Fock hybrid method, i.e., the B3LYP functional and the multireference-averaged quadratic coupled cluster approach. The global minimum is linear FeNO($^2\Delta$), which is not adiabatically connected to the neutral ground-state fragments Fe and NO. Side-on and oxygen-bound isomers have low barriers for rearrangement; however, they might be stabilized because of ligand effects. Inserted OFeN($^4A''$) is kinetically stable, although it lies considerably higher in energy than the other isomers. The calculations indicate near-degenerate ground states for all isomers. We discuss the implications for the reported experimental observations. Furthermore, the findings are rationalized using valence bond and molecular orbital theories.

Introduction

Surprisingly, nitric oxide NO, a highly toxic radical, plays an essential role in biochemistry; in the context of the regulatory mechanism of vasorelaxation, its binding to hemoglobin is of crucial relevance.[1] Light-induced isomerizations of [FeNO]-containing complexes, such as sodium nitroprusside, have received interest because of possible technical applications for information storage systems.[2] Thus, it is not surprising that ligand-free FeNO itself has become a subject of basic research. Recently, a matrix infrared (IR) spectroscopy study of the reaction of laser-ablated Fe atoms with some small molecules including NO has been published.[3] The authors also reported their calculations, using density functional theory (DFT),[4] on the elusive ternary iron nitride oxide molecule, OFeN, to support the experimental assignments, which were based on vibration frequencies and isotopic shifts. In passing, we mention gas-phase studies of the kinetics of excited-state depletion for first-row transition metals by NO.[5] Unfortunately, the results for iron are not published yet because of experimental difficulties.[6]

Nowadays, ab initio theory offers an alternative supplemental approach to gain insight into such systems.[7] However, the accurate theoretical treatment of open-shell compounds still constitutes a fundamental challenge to state-of-the-art quantum chemistry. It is not only a problem of the high level of theory that has to be applied to reach a qualitative picture but may be attributed to the fundamental complexity, when compared to first- and second-row-element-containing compounds. This is also reflected in the experimental studies, where the interpretations of the puzzling data constitute a challenge. The causes of these problems are rather well understood: (1) many intrinsic low-lying open-shell states of the transition metals, (2) very distinct binding properties of the 4s and 3d electrons, and (3) low ionization energies. These factors give rise to a manifold of low-lying states in the molecules concerned. As such, the complexity primarily can be ascribed to near-degeneracy effects, which are still rather challenging with regard to the computational costs. Additionally, various unusual binding mechanisms, which are beyond ordinal chemical terminology, such as bond order and oxidation state, can give rise to an amazing stability of isomers and states, unexpected at first glance.[8] Thus, careful systematic studies are needed to reach a sufficiently realistic portrait of transition metal compounds in order to be useful for explaining their physical and chemical properties. The obvious strength of theory is the rationalization of data on an atomic basis, which through generalization may lead to predictive models.[9,10] Additionally, details can be explored, which are hitherto inaccessible by spectroscopic experimental methods.[10−13]

In the present paper we report a systematic study of the isomers of [Fe, N, O] to predict the global minimum, their ground states, and corresponding barriers for interconversions on various potential energy hypersurfaces. This work is an extension of our report on FeN.[14] For geometry optimizations we apply an economic B3LYP[15] DFT/HF hybrid approach, which has been repeatedly shown to result in a reasonable description of structures and energies.[11,16] For a more quantitative picture and especially for the verification of the energies, the recently developed internally contracted[17] averaged quadratic coupled cluster approach (AQCC),[18] a size-consistent extension[19] of the well-known multireference configuration interaction method, has been applied. In the present system the AQCC method is probably the most complete treatment of correlation energy yet possible. This study gives insight into the interesting physical properties of this important system and additionally allows the critical examination of the performance of the applied methods.

Computational Details

Calculations have been performed similarly to those described in the previous paper on FeN.[14] For geometry optimizations we applied the economic B3LYP functional[15] with standard 6-311G* basis sets as implemented in the Gaussian94 program.[20] This level of theory has been shown to result in geometric structures similar to those from highly correlated molecular orbital methods. We did not choose the alternative CASSCF geometry optimizations, since that particular method is considerably more difficult to use and, furthermore, it tends to overestimate bond length in transition metal systems because of the lack of dynamic correlation.[21]

Flexible atomic natural orbital (ANO) basis sets have been applied for the multireference-based single-point calculations

S1089-5639(98)00523-4 CCC: $15.00
Published on Web 04/23/1998

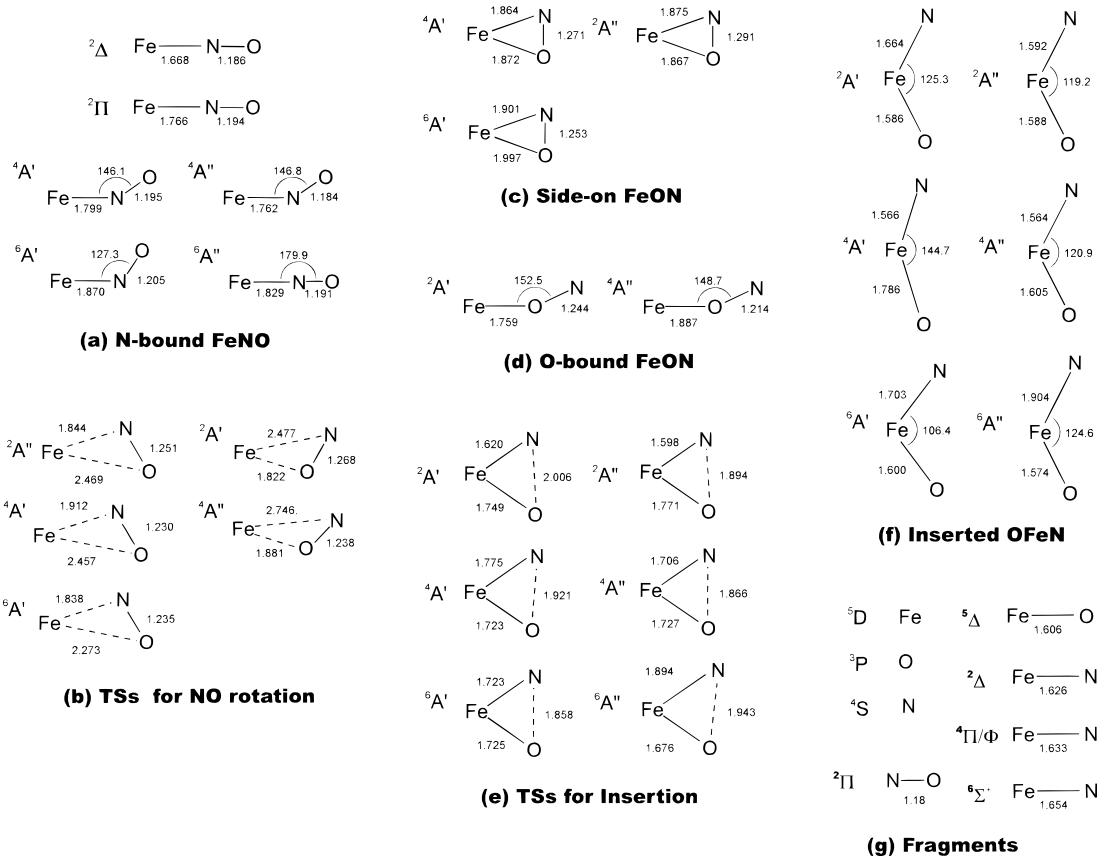

Figure 1. Calculated structures of [Fe, N, O] isomers and fragments.

using the Molpro94 program package.[22] The metal was described by Pou-Amerigo's (21s15p10d6f4g)/[7s6p5d4f2g] basis set.[23] For nitrogen and oxygen we applied Widmark's (14s9p4d3f)/[6s5p3d2f] basis sets.[24] The 1s2s2p3s3p(Fe), 1s2s(O), and 1s2s(N) electrons have been treated as inactive in the CASSCF calculations. Because of program limitations, the highest a′ valence orbital, i.e., a delocalized antibonding in-plane orbital, was excluded from the active space generated by the 4s3d(Fe), 2p(O), and 2p(N) valence orbitals. Thus, the configuration state functions (CSF, typically 10 000) were created by filling 15 electrons in eight a′ and four a″ orbitals. We will note in the discussion when this approximation has influence on the reliability of the calculations. All CSFs having a coefficient larger than 0.05 in the CASSCF were included as reference configurations (ca. 90 CSFs) in the internally contracted AQCC computations, and all 19 valence electrons have been correlated. This results in typically 4 500 000 contracted configurations corresponding to about 200 000 000 uncontracted configurations. To warrant proper symmetry, isolated atoms and molecular fragments of degenerate point groups have been calculated using a state-averaged procedure for the corresponding roots in C_{2v} or D_{2h}, which has been described in detail in a preceding publication.[14]

No corrections for relativistic effects,[25] core-valence correlation, zero-point vibration energy, imperfect basis sets,[26] and incompleteness of the correlation treatment[27] have been applied. When dissociation energies are corrected, these corrections could sum up to about 10 kcal/mol but are less important for relative energies. Nevertheless, theoretical studies of transition metal systems seldom reach spectroscopic accuracy and thus the reported values should still be regarded as semiquantitative and suggestive for the interpretation of the experimental data.

Results and Discussion

In the present paper we report results for the states possessing doublet to sextet multiplicity of [Fe, N, O]. Numerous isomers, namely, nitrosyl iron FeNO, inserted iron nitride oxide OFeN, oxygen-bound isomers FeON, and cyclic or side-on forms, have been characterized. In addition, all interconnecting transition structures have been examined. Parts a−f of Figure 1 display the geometries of these stationary points on the potential energy hypersurfaces (PES), and Figure 1g shows the fragments. In Table 1 the corresponding calculated frequencies, relative energies with respect to isolated ground-state Fe(^{5}D) and NO($^2\Pi$) at the B3LYP level, and refined AQCC single-point energies for the low-lying structures are shown. From these calculations we can derive the qualitative adiabatic PESs scheme shown in Figure 2.

Global Minimum: Nitrosyl Iron FeNO. The ground states of Fe ($4s^23d^6$; ^{5}D) and NO ($^2\Pi$) give rise to quartet and sextet states for the unified molecule. However, the calculations indicate that the global minimum is nitrogen-bound FeNO in the low-spin $^2\Delta$ state, which is asymptotically connected to the first excited ^{3}F state of iron located 20 kcal/mol higher in energy. Thus, the ground-state molecule does not form the expected simple single covalent σ bond between a quintet Fe atom and a doublet NO$^\bullet$ radical, which has quartet multiplicity and a bent structure (see below).

Figure 3 illustrates the molecular orbitals generated from the orbitals of the fragments for which the ground-state occupation is indicated by arrows. At the dissociation limit five electrons occupy the 10σ, 11σ, and 12σ orbitals[28] constituting of 4s(Fe), 3dσ(Fe), and the σ-bonding orbital of NO. However, the main configuration of the FeNO $^2\Delta$ state is $10\sigma^2\ 11\sigma^2\ 3\pi^4\ 4\pi^4\ 1\delta^3$. Hence, the 12σ orbital is not occupied, but we can locate the

TABLE 1: Relative Energies (E_{rel}) with Respect to Isolated Ground-State Fe (^{5}D) and NO ($^2\Pi$) and Harmonic Frequencies (ω) of [Fe, N, O] Stationary Points

structure	state	ω/cm^{-1} B3LYP	E_{rel} kcal/mol B3LYP	E_{rel} kcal/mol AQCC
N-bound	$^2\Delta$	162, 508, 1815	−21	−14
	$^2\Pi$	i629, 117, 479, 1741[a]	0	
	^{4}A′	179, 463, 1722	−11	−12
	^{4}A″	230, 462, 1708	−12	−12
	^{6}A′	201, 367, 1571	2	5
	^{6}A″	80, 447, 1745	5	−1
O-bound	^{2}A′	97, 520, 1430	3	
	^{4}A″	128, 351, 1309	6	
side-on	^{2}A″	459, 474, 1263	22	
	^{4}A′	433, 512, 1331	2	2
	^{6}A′	345, 407, 1308	3	
TS rotation	^{2}A′	i172, 546, 1280	5	
	^{2}A″	i238, 485, 1442	32	
	^{4}A′	i199, 491, 1496	9	
	^{4}A″	i136, 443, 1314	7	
	^{6}A′	i279, 518, 1432	5	
inserted	^{2}A′	248, 555, 991	17	30
	^{2}A″	270, 520, 989	14	16
	^{4}A′	52, 425, 711	34	
	^{4}A″	332, 818, 952	13	10
	^{6}A′	239, 601, 923	26	29
	^{6}A″	122, 494, 982	40	
TS insertion	^{2}A′	i482, 571, 738	61	70
	^{2}A″	i628, 626, 837	50	61
	^{4}A′	i716, 475, 740	58	
	^{4}A″	i646, 544, 750	46	45
	^{6}A′	i715, 528, 814	46	44
	^{6}A″	i564, 506, 812	52	

[a] FeNO $^2\Pi$ is a crossing point of ^{2}A′ and ^{2}A″ PESs (see Results and Discussion).

missing electron in the 8π orbital ($8\pi^4$). This particular configuration can be assigned to the higher-lying Fe(^{3}F; $4s^1\ 3d_\sigma^1\ 3d_\pi^3\ 3d_\delta^3$) and NO($^2\Pi$; $2\pi^1$) asymptote. Furthermore, ionic dissociation limits, e.g., Fe^+(^{4}F; $4s^0\ 3d_\sigma^2\ 3d_\pi^2\ 3d_\delta^3$) and NO^- ($^3\Sigma^-$; $2\pi^2$) states, also match the symmetry requirements, and thus, the $^2\Delta$ wave function can be stabilized owing to charge transfer (CT). Although this exit channel is located considerably higher in energy, for the combined molecule the CT can be rationalized by a simple electrostatic model;[29] taking into account the ionization energy of Fe and the electron affinity of NO and assuming a nonbonding ground-state PES, the Coulomb attraction of the ions ($1/r_{Fe^+-NO^-}$) can overweigh the costs for charge separation for Fe−NO distances as large as ca. 2.5 Å. Additionally, in contrast to the ground-state asymptote, the ionic fragments favor a straightforward orbital interaction for FeNO. The spatially large 4s(Fe) orbital, which is doubly occupied in the ground state of neutral iron, is now free as an accepting orbital for charge donation from the NO^- σ orbital, which has strong lone-pair character on nitrogen. The low-lying 10σ bonding orbital shows this composition, and hybridization of 4s and $3d_\sigma$ at the iron atom can be observed. The occupied 11σ orbital, the nonbonding sd hybrid orbital on iron, is polarized out of the σ axis of the molecule to minimize electrostatic repulsion. The antibonding 12σ orbital remains unoccupied. In addition, the fully occupied 4π orbitals created by the half-filled Fe^+ $3d_\pi$ orbitals and NO^- π^* orbitals form a pair of covalent Fe−N π bonds. Finally, there remains one unpaired $3d_\delta$ electron in the iron d_δ^3 configuration, resulting in doublet multiplicity.

Obviously, the pure ionic picture alone is too simple, since we can expect strong mixing with the lower-lying asymptotes, e.g., Fe(^{3}F) + NO($^2\Pi$), that give rise to multiple avoided crossings on this doublet PES. Actually, the natural bond orbital population analysis indicates a charge transfer of about 0.5 e, hence pointing to a mixture of neutral and ionic asymptotes. Additionally, the short bond length of 1.67 Å (Figure 1a) and the linearity of FeNO($^2\Delta$) reflect the multiple-bond character between Fe and N as illustrated above. The calculated harmonic frequencies of the stretching modes are rather high (Table 1), consistent with this description. For bending, only one harmonic frequency is given in Table 1, in line with the Renner−Teller theorem, that showed in general the ^{2}A′ and ^{2}A″ PESs resulting from a $^2\Delta$ state have equal harmonic force constants.

In contrast, for the excited $^2\Pi$ state the analytical calculation reveals one imaginary frequency (a′ mode) and one real frequency (a″ mode) for bending. It implies that one of the Renner−Teller splitting states is linear and the other is bent and that the bent ^{2}A′ is lower than the linear $^2\Pi$ state. We did not succeed in locating this ^{2}A′ minimum; not surprisingly, the B3LYP computations converged to the $^2\Delta$ state, which corresponds to the minimum on the lowest-lying ^{2}A′ and ^{2}A″ PESs. Here, the single-determinant approach clearly finds its limitations.[30] A detailed study at the AQCC level would go beyond the scope of the present paper.

For quartet spin multiplicity we found low-lying bent FeNO structures, ^{4}A′ and ^{4}A″. They are easily described by covalent single bonds (ca. 1.8 Å) between the singly occupied sd hybrid orbital on the iron center and the singly occupied π^* orbital on NO, which has its maximum amplitude on the nitrogen center. However, the σ bond is strongly polarized toward the electronegative ligand, and thus, the CT asymptotes also play a significant role in the quartet states. Consequently, the wave functions show a very high degree of multireference character. The bending of about 150° can be rationalized by a balance of pure covalent σ bonding, which should prefer ca. 90° or 120° if sp^2 hybridization on nitrogen is assumed, and the ionic complex having additional multiple bond character, which is expected to be linear.

For sextet FeNO the electrons of the ground-state asymptote, Fe ^{5}D and NO $^2\Pi$, formally remain uncoupled. The rather large Fe−N distances for the ^{6}A′ and ^{6}A″ FeNO isomers reflect this character. However, in the ^{6}A′ state the bending structure points toward covalent contributions, which can only result from configuration interactions with other low-lying exit channels.

The binding energy of the global minimum $^2\Delta$ FeNO relative to ground-state Fe and NO amounts to only 14 kcal/mol at the AQCC level of theory. Bent quartet isomers ^{4}A″ and ^{4}A′, correlated to the ground-state asymptote, are calculated to be less stable by 2 kcal/mol. The sextet isomers are higher in energy, but ^{6}A″ is still located just below the dissociation products at this level of theory. To the best of our knowledge, no experimental dissociation energy has been reported yet. Nevertheless, the low stabilization energy reflects the unfavorable binding properties of the ground-state $4s^2$ configuration of the metal.

Results from the B3LYP computations show a reasonable qualitative agreement with the AQCC calculations. The largest observed deviation is 7 kcal/mol in the case of the $^2\Delta$ state, and the stabilization for the high-spin states seems to be slightly underestimated. This follows the general trend of DFT calculations as repeatedly discussed in the literature.[31] The calculated frequencies of about 1700−1800 cm^{-1} for the NO stretching vibrations for the low-lying doublet and quartet isomers are in line with the experimental assignments of the matrix IR study by Andrews et al.[3] Spectra observed in this wavenumber region might indeed indicate the presence of more than one electronic

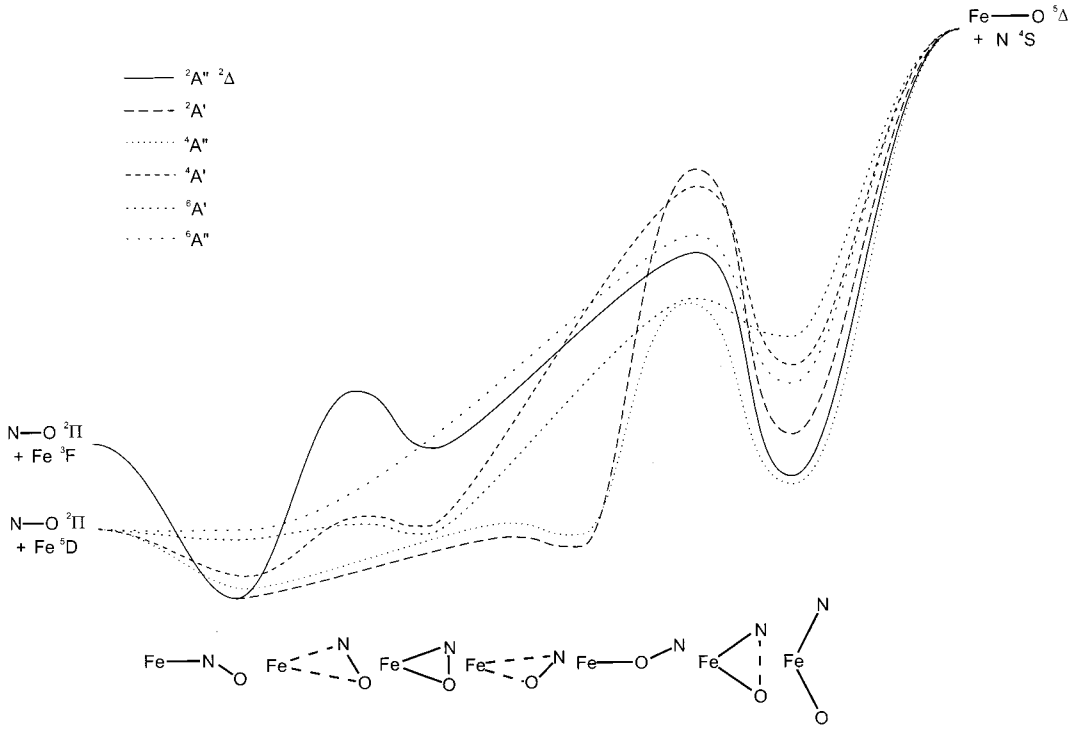

Figure 2. Schematic potential energy hypersurfaces for [Fe, N, O].

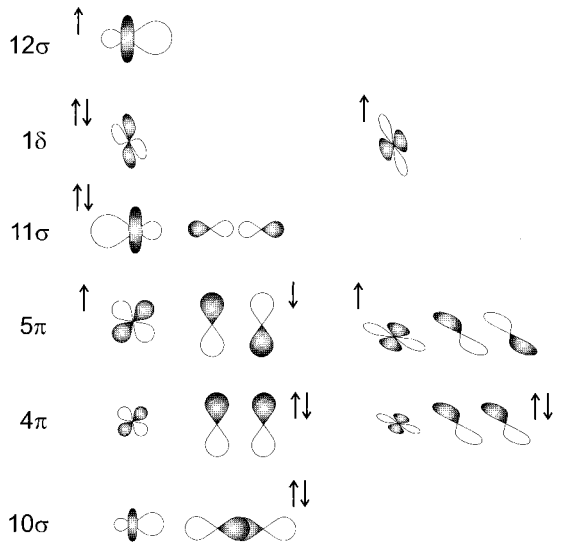

Figure 3. Qualitative molecular orbitals for linear end-on FeNO. The arrows indicate the occupation in the ground-state fragments Fe(^{5}D) and NO(^{2}P).

state (or isomer) in the experiment due to the near-degeneracy of $^2\Delta$, ^{4}A′, and ^{4}A″. Finally, we note the good agreement of our calculated Fe−N distance of 1.67 Å for the $^2\Delta$ low-spin state with the reported value by Carducci et al.[2] from a diffraction study of an $Fe(CN)_5NO$ closed-shell complex, which also has a linear FeNO unit.

Side-on Isomers vs Oxygen-Bound FeON. Carducci et al.[2] have shown evidence for a long-living, metastable oxygen-bound complex in the solid state and even a third isomer, which might be assigned to a side-on conformation. Actually, our geometry optimizations for bare [Fe, N, O] confirm minima for both types of isomers (parts c and d of Figure 1). Interestingly, for a given spin multiplicity, they alternatively appear on the potential energy hypersurfaces of distinct spatial symmetry, A′ and A″, respectively. The only exception is the ^{6}A″ state where we did not find the anticipated O-bound isomer. All attempts led to dissociation. Nevertheless, this implies electronic effects, which we analyze below.

For oxygen-bound FeON a molecular orbital correlation diagram similar to Figure 3 for FeNO can be applied. Some quantitative differences result from the size of coefficients for the σ_{NO} and π^* orbitals at the iron-coordinating atom of NO. For both orbitals the coefficients on O are smaller than on N. Thus, the orbital interaction with the metal is weaker in the oxygen-bound molecule than in the nitrogen-bound isomer. Hence, in the first place the weaker overlap is responsible for stabilization energies of FeON that are lower than those of FeNO (Table 1). The overlap can be slightly increased by bending the molecule, since this symmetry relaxation allows mixing of σ_{NO} and π^*(NO). The stable O-bound isomers, ^{2}A′ and ^{4}A″, are shown in Figure 1d. The structures imply the usual sp^2 hybridization for the oxygen atom and a single bond to the metal (around 1.8 Å).

The side-on interaction is quite different, which is shown schematically in Figure 4. Since both atoms simultaneously touch the metal, the nodal structures of the orbitals along the bonding axis of NO become significant for the overlap to the metal orbitals. More importantly, the in-plane NO orbitals (a′ components) strongly interact with the metal a′ orbitals, whereas the overlap is less favorable for the out-of-plane a″ components. Consequently, the two $3d_{a''}$(Fe) and two a″ orbitals on NO (out-of-plane π and π^*) form two bonding molecular orbitals (3a″ and 4a″) and two formally antibonding but rather low-lying orbitals (5a″ and 6a″). We found that the stable side-on isomers have the following main configurations with maximum occupation of these out-of-plane a″ orbitals for the given multiplicity: ^{2}A″($15a'^2\ 16a'^2\ 5a''^1$), ^{4}A′($15a'^2\ 16a'^1\ 5a''^1\ 6a''^1$), and ^{6}A′($15a'^1\ 16a'^1\ 5a''^1\ 6a''^1\ 17a'^1$). Obviously, changing the spatial symmetry, i.e., excitation from a″ into a′, causes the side-on structures to no longer be stable minima but transition structures (Figure 1b) leading to the end-on O-bound arrangements. A

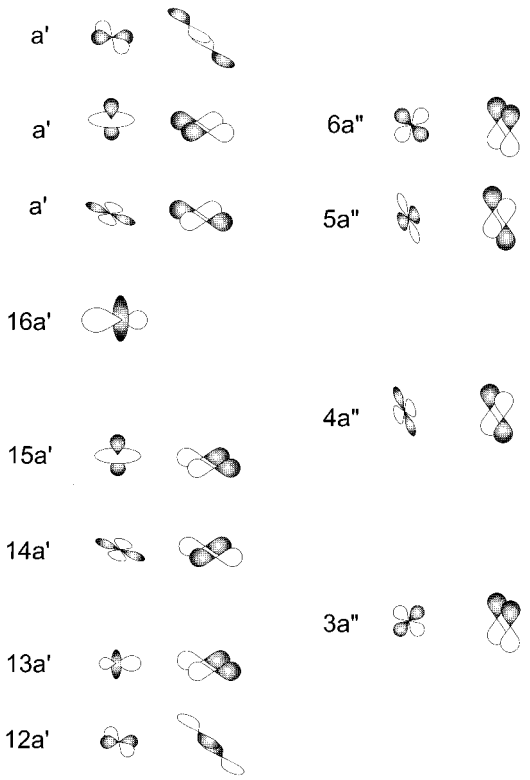

Figure 4. Qualitative molecular orbitals for side-on FeNO. The left column shows the in-plane orbitals and the right column the out-of-plane orbitals.

simple explanation for this fact might be that the system relaxes by opening the cyclic structure in order to diminish the greater electron−electron repulsion in the in-plane non- or antibonding orbitals.

Stability of Side-on and Oxygen-Bound Isomers. As shown in Table 1 and Figure 2, all states of the side-on structures and the oxygen-bound end-on $^4A''$ isomer are computed to lie in the energy range of their asymptotic exit channels, which indicates overall rather unfavorable interactions. In addition, barriers for direct dissociation can generally be expected as very small (about a few kcal/mol), and thus, these states might not be observable in a finite temperature experiment. Only O-bound FeON $^2A'$ is considerably more stabilized and located near the ground-state asymptote to which the dissociation is not spin-allowed. However, spin−orbit coupling will permit a slow transition to this high-spin PES.[10]

Furthermore, for the kinetic stability also the barriers for rotation of the NO ligand leading to the lower-lying N-bound isomers are decisive. The optimized transition structures displayed in Figure 1b have the expected structural features (the left side of Figure 2 shows the correlation between these TSs and the isomers). For all energetically lower-lying isomers, including $^2A'$ FeON, the computations reveal only small barriers of about 2 kcal/mol for rotations to the more stable FeNO structures. Only the more energy-demanding $^2A''$ TS for the side-on isomer might be high enough to prevent this kind of rearrangement, but as discussed above, this state is not very stable with respect to dissociation. Thus, one could expect that none of these isomers are very likely to be trapped experimentally.

However, matrix and ligand effects might considerably stabilize the low-spin PESs and, hence, side-on and oxygen-bound isomers.[13] This has been shown in the diffraction studies of photoexcited $Na_2[Fe(CN)_5NO]\cdot H_2O$ crystals where all three configurations were observed.[2] In the matrix IR experiments, Andrews et al. found weak red-shifted signals in the area of our computed frequencies (∼1300 cm^{-1}), but they interpreted them as NO^- anions weakly interacting with Fe^+.[3] The NO^- anion is known to absorb in this frequency range.[32] Consequently, the low-frequency signals could be explained by a reduced NO bond strength accompanying CT to the π^* orbital. However, we did not find indications of a higher degree of CT neither for the side-on nor the O-bound isomers when compared with end-on FeNO $^2\Delta$. Rather, the low frequencies can be explained solely by the bonding to the metal. Hence, with the assumption that matrix effects stabilize these isomers, they offer an alternative explanation for the observed signals.

Insertion Product: The Elusive OFeN Isomer. We also calculated the recently detected inserted OFeN molecule.[3] In Figure 1f the optimized geometries for the states are shown. The Fe−N and Fe−O bonds in the two lowest-lying isomers, $^4A''$ and $^2A''$, are as short as 1.6 Å. This bond length is typical also for the binary species shown in Figure 1g. For the higher states ($^2A'$, $^4A'$, $^6A'$, and $^6A''$) the distances increase gradually up to 1.9 Å, reflecting weaker bonding in the underlying electron configurations. The calculated frequencies for the lowest $^4A''$ state (N−Fe stretch, 952 cm^{-1}; Fe−O stretch, 818 cm^{-1}) show good agreement with the experimental assigned values of 971 and 796 cm^{-1}. Reliable calculations of frequencies in open-shell transition metal compounds, however, are not as straightforward as for molecules of first- and second-row atoms, and the very good conformity might be accidental.

Hence, to ascertain our assignment of the ground state of the inserted isomer and to explain the relative stability of the states, the orbital interactions of the three atoms are examined. Similar symmetry considerations as for the side-on isomers were assumed (Figure 4). However, the ordering and shape of the molecular orbitals differ considerably, since they stem from the interaction of the metal with separated atomic O and N. The orbitals are quite complex in shape; i.e., strong mixing of all a′ and a″ orbitals, respectively, can be observed. Nevertheless, we try to present a sound but very simplified description. The bending of around 120° implies sd^2 hybridization on the metal. Two iron hybrid orbitals are pointing toward oxygen and nitrogen, respectively, approaching from the *x* direction in the *xy* plane, and the third is pointing in the opposite direction. We begin with the two low-lying a′ molecular orbitals (12a′ and 13a′) representing two σ bonds formed by interactions of one iron sd^2 hybrid orbital, and a p orbital on N or O pointing to the iron center (mixture of p_x and p_y). Additionally, we have two in-plane, more π-type bonding a′ orbitals (14a′ and 15a′) created from the iron $d_{y^2-x^2}$ orbital and the nitrogen or oxygen p orbitals orthogonal to the two σ bonds. Furthermore, there are two out-of-plane π-bonding a″ orbitals (3a″ and 4a″) from the in-phase interactions of the iron d_{zy} and d_{zx} orbitals with p_z(O) and p_z(N). These orbitals will be filled first, and the three remaining electrons will first occupy the third nonbonding sd^2 hybrid orbital on Fe (16a′) and the following low-lying antibonding π^* orbitals, in-plane (17a′) and out-of-plane (5a″). The high-spin-coupled $16a'^1\ 5a''^1\ 17a'^1$ configuration corresponds to the lowest computed $^4A''$ state.

Possible configurations of the alternative quartet state $^4A'$ are less advantageous, since their prerequisite is occupation of two π^* orbitals having the same symmetry. For the doublet states, one of the antibonding electrons in 17a″ or 5a″ can be placed into the lower-lying iron sd^2 hybrid orbital (16a′), leading to $^2A'$ or $^2A''$ symmetry. However, according to our calculations, for both states the loss of exchange energy slightly overcom-

pensates this kind of stabilization, and the states are slightly higher in energy than the $^4A''$ state. Finally, for sextet states excitations out of the bonding orbitals are necessary and obviously the exchange energy gain is not sufficient to stabilize these unfavorable situations. Thus, the lowest calculated quartet state $^4A''$ represents the configuration with maximum occupation of bonding orbitals and maximal high-spin-coupled electrons in the non- or antibonding space and it is plausible that this is the ground state.

Stability of OFeN. For the OFeN isomer the B3LYP and AQCC calculations show a qualitative agreement of the relative energies. We observe the largest deviation between both levels ($^2A'$: $\Delta E = 13$ kcal/mol). However, we note that in these cases the AQCC calculations are slightly less reliable than for the other structures, since for OFeN we found external configurations with weights slightly larger than the reference selection threshold of 0.05. These configurations describe excitations into orbitals generated by the 4p orbitals on iron and the highest a′ valence orbital that we have treated as virtual in the CASSCF. We have not been able to include them in the active space because of computational limitations. However, the reasonable consistency of the B3LYP and AQCC values indicates that no larger error is introduced because of this restriction.

In contrast to our calculations Andrews et al.[3] found the doublet multiplicity of 3 kcal/mol to be more stable than the quartet multiplicity (they did not report the spatial symmetry), which might reflect the well-known bias of DFT approaches to favor low-spin configurations due to the underestimation of exchange energy loss accompanying spin-pairing. The same tendency becomes even more visible in their rather high value of 96 kcal/mol for the Fe−N bond dissociation energy for this isomer. According to our calculations, the corresponding energy to produce FeO($^5\Delta$) and N(^{4}S) from OFeN($^4A''$) amounts to only 58 kcal/mol at the AQCC level of theory and 66 kcal/mol using the DFT/HF hybrid functional. The latter suffers less severely from the discussed DFT shortcoming. OFeN is also stable with respect to the other direct dissociation channel, FeN $^2\Delta$ and O ^{3}P, which is located higher in energy (AQCC, 31 kcal/mol; B3LYP, 26 kcal/mol). However, it is calculated to be 24 kcal/mol higher than the global minimum end-on FeNO $^2\Delta$, and the process yielding isolated ground-state Fe and NO is exothermic by 10 kcal/mol.

To explain why this isomer is observed experimentally, we also have to analyze the rearrangement to the more stable isomers, i.e., the reductive elimination step or, backward, oxidative insertion of Fe into the NO bond. Figure 1e displays the corresponding stationary points found on the PESs; the N−O distances are as long as 1.9 Å and the Fe−N and Fe−O distances are between those in the complex and in the inserted species. The lowest-lying TSs have $^6A'$ and $^4A''$ symmetry and are located about 45 kcal/mol above the global minimum FeNO $^2\Delta$ and are ca. 35 kcal/mol higher than the most stable OFeN species having $^4A''$ symmetry. Thus, the OFeN → FeNO rearrangement is hampered by significantly high barriers, and thus, it is not surprising that both isomers could be observed under the low-temperature conditions of the matrix IR experiment.

Final Remarks

In summary, Figure 2 shows that the chemistry of Fe and NO is slightly more complex than usually considered for nonmetal systems, which often can be described by only one PES. The global minimum, FeNO, is most probably not derived from the ground states of the lowest-lying fragments. Additionally, we found oxygen-bound and side-on isomers, which have not been considered in a previous report.[3] Furthermore, the calculations indicate near-degenerate ground states for the isomers. We discussed the implications for the interpretation of the available experimental data. To go beyond that, simple MO and VB considerations have been used to understand the physical properties. Finally, we note that along the lowest energy paths for the discussed isomerizations some curve crossings occur, which may have hardly predictable consequences for the unknown kinetic and dynamic aspects of the reaction of iron with NO. We hope that our complementary study is helpful for forthcoming experiments.

Acknowledgment. A postdoctoral fellowship of the Japanese Society for the Promotion of Science, which made possible the stay of A.F. at IMS, is deeply appreciated. The present work was partially supported by a Grant-in-Aid for Scientific Research (No.09304057) by the Japanese Ministry of Education, Science, and Culture. We acknowledge the provision of computational resources from the computer center of IMS. A.F. especially thanks T. Tsurusawa for continuous technical support.

References and Notes

(1) Perutz, M. F. *Nature* **1996,** *380*, 205.
(2) Carducci, M. D.; Pressprich, M. R.; Coppens, P. *J. Am. Chem. Soc.* **1997**, *119*, 2669.
(3) Andrews, L.; Chertihin, G. V.; Citra, A.; Neurock, M. *J. Phys. Chem.* **1996,** *100*, 11235.
(4) Parr, R. G.; Yang, W. *Density-Functional Theory of Atoms and Molecules*; Oxford University Press: New York, 1989.
(5) Matsui, R.; Senba, K.; Honma, K. *J. Phys. Chem. A* **1997,** *101*, 179.
(6) Honma, K. Private communication.
(7) Ohanessian, G.; Goddard, W. A., III. *Acc. Chem. Res.* **1990,** *23*, 386. Koga, N.; Morokuma, K. *Chem. Rev.* **1991,** *91*, 823.
(8) Schröder, D.; Fiedler, A.; Schwarz, J.; Schwarz, H. *Inorg. Chem.* **1994,** *33*, 5094. Schröder, D.; Fiedler, A.; Herrmann, W. A.; Schwarz, H. *Angew. Chem., Int. Ed. Engl.* **1995,** *34*, 2517.
(9) Hoffmann, R. *Angew. Chem., Int. Ed. Engl.* **1982**, *21*, 711. Carter, E. A.; Goddard, W. A., III. *J. Phys. Chem.* **1988,** *92*, 2109. Armentrout, P. B. *Science* **1991,** *251*, 175.
(10) Fiedler, A.; Schröder, D.; Shaik, S.; Schwarz, H. *J. Am. Chem. Soc.* **1994**, *116*, 10734. Shaik, S.; Danovich, D.; Fiedler, A.; Schröder, D.; Schwarz, H. *Helv. Chim. Acta* **1995,** *78*, 1393.
(11) Veldkamp, A.; Frenking, G. *J. Am. Chem. Soc.* **1994**, *116*, 4937. Yoshizawa, K.; Shiota, Y.; Yamabe, T. *Chem. Eur. J.* **1997**, *3*, 1161.
(12) Holthausen, M. C.; Fiedler, A.; Schwarz, H.; Koch, W. *Angew. Chem., Int. Ed. Engl.* **1995**, *34*, 2282. Holthausen, M. C.; Fiedler, A.; Schwarz, H.; Koch, W. *J. Phys. Chem.* **1996**, *100*, 6237.
(13) Fiedler, A.; Schröder, D.; Schwarz, H.; Tjelta, B. L.; Armentrout, P. B. *J. Am. Chem. Soc.* **1996**, *118*, 5047. Fiedler, A.; Schröder, D.; Zummack, W.; Schwarz, H. *Inorg. Chim. Acta* **1997**, *259*, 227.
(14) Fiedler, A.; Iwata, S. *Chem. Phys. Lett.* **1997,** *271*, 143.
(15) Becke, A. D. *J. Chem. Phys.* **1993**, *98*, 5648.
(16) Holthausen, M. C.; Mohr, M.; Koch, W. *Chem. Phys. Lett.* **1995**, *240*, 245. Ricca, A.; Bauschlicher, C. W., Jr. *Chem. Phys. Lett.* **1995**, *245*, 150.
(17) Werner, H.-J.; Knowles, P. J. *Theor. Chim. Acta* **1990**, *78*, 175.
(18) Szalay, P. G.; Bartlett, R. P. *Chem. Phys. Lett.* **1993,** *214*, 481.
(19) Gdanitz, R. J.; Ahlrichs, R. *Chem. Phys. Lett.* **1988**, *143*, 413.
(20) Frisch, M. J.; Trucks, G. W.; Schlegel, H. B.; Gill, P. M. W.; Johnson, B. G.; Robb, M. A.; Cheeseman, J. R.; Keith, T.; Petersson, G. A.; Montgomery, J. A.; Raghavachari, K.; Al-Laham, M. A.; Zakrzewski, V. G.; Ortiz, J. V.; Foresman, J. B.; Cioslowski, J.; Stefanov, B. B.; Nanayakkara, A.; Challacombe, M.; Peng, C. Y.; Ayala, P. Y.; Chen, W.; Wong, M. W.; Andres, J. L.; Replogle, E. S.; Gomperts, R.; Martin, R. L.; Fox, D. J.; Binkley, J. S.; Defrees, D. J.; Baker, J.; Stewart, J. P.; Head-Gordon, M.; Gonzalez, C.; Pople, J. A. *Gaussian 94*, Revision B.2; Gaussian, Inc.: Pittsburgh, PA, 1995.
(21) Fiedler, A.; Hrušák, J.; Koch, W.; Schwarz, H. *Chem. Phys. Lett.* **1993**, *211*, 242.
(22) Werner, H.-J.; Knowles, P. J. *Molpro94*; University of Sussex: U.K., 1994 with contributions from the following: Almlöf, J.; Amos, R. D.; Deegan, M. J. O.; Elbert, S. T.; Hampel, C.; Meyer, W.; Peterson, K.; Pitzer, R.; Stone, A. J.; Taylor, P. R.

(23) Pou-Amerigo, R.; Merchan, M.; Nebot-Gill, I.; Widmark, P.-O.; Roos, B. O. *Theor. Chim. Acta* **1995**, *92*, 149.

(24) Widmark, P.-O.; Malmqvist, P.-A.; Roos, B. O. *Theor. Chim. Acta* **1990,** *75*, 291.

(25) Pyykkö, P. *Chem. Rev.* **1988,** *88*, 563.

(26) Boys, S. F.; Bernardi, F. *Mol. Phys.* **1970**, *19*, 553.

(27) Siegbahn, P. E. M.; Blomberg, M. R. A.; Svensson, M. *Chem. Phys. Lett.* **1994,** *223*, 35. Siegbahn, P. E. M.; Svensson, M.; Boussard, P. J. E. *J. Chem. Phys.* **1995,** *102*, 5377.

(28) The two lowest-lying valence molecular orbitals ($C_{\infty v}$, 8σ, 9σ; and C_s, 10a′, 11a′) have almost pure $2s^2$(O) and $2s^2$(N) character and are omitted in the discussions.

(29) Dubois, L. H.; Gole, J. L. *J. Chem. Phys.* **1977,** *66*, 779.

(30) Additionally, in the single-determinant approach, strong mixing with a quartet-coupled $^4\Pi(\delta^2\pi^3)$ state takes place (see ref 14).

(31) Ziegler, T.; Li, J. *Can. J. Chem.* **1994,** *72*, 783.

(32) Spence, D.; Schulz, G. J. *Phys. Rev. A.* **1971**, *3*, 1968.